

SANDIA REPORT

SAND98-8209 • UC-401

Unlimited Release

Printed December 1997

RECEIVED
DEC 15 1997
OSTI

Efficient Broadband Second-Harmonic Generation by Dispersive Achromatic Nonlinear Conversion Using Only Prisms

DISTRIBUTION OF THIS DOCUMENT IS UNLIMITED

B.A. Richman, S.E. Bisson, R.P. Trebino

MASTER

Prepared by
Sandia National Laboratories
Albuquerque, New Mexico 87185 and Livermore, California 94550

Sandia is a multiprogram laboratory operated by Sandia Corporation,
a Lockheed Martin Company, for the United States Department of
Energy under Contract DE-AC04-94AL85000

Approved for public release; distribution is unlimited.



Sandia National Laboratories

Issued by Sandia National Laboratories, operated for the United States Department of Energy by Sandia Corporation.

NOTICE: This report was prepared as an account of work sponsored by an agency of the United States Government. Neither the United States Government nor any agency thereof, nor any of their employees, nor any of their contractors, subcontractors, or their employees, makes any warranty, express or implied, or assumes any legal liability or responsibility for the accuracy, completeness, or usefulness of any information, apparatus, product, or process disclosed, or represents that its use would not infringe privately owned rights. Reference herein to any specific commercial product, process, or service by trade name, trademark, manufacturer, or otherwise, does not necessarily constitute or imply its endorsement, recommendation, or favoring by the United States Government, any agency thereof, or any of their contractors or subcontractors. The views and opinions expressed herein do not necessarily state or reflect those of the United States Government, any agency thereof, or any of their contractors.

Printed in the United States of America. This report has been reproduced directly from the best available copy.

Available to DOE and DOE contractors from
Office of Scientific and Technical Information
P.O. Box 62
Oak Ridge, TN 37831

Prices available from (615) 576-8401, FTS 626-8401

Available to the public from
National Technical Information Service
U.S. Department of Commerce
5285 Port Royal Rd
Springfield, VA 22161

NTIS price codes
Printed copy: A03
Microfiche copy: A01

DISCLAIMER

Portions of this document may be illegible electronic image products. Images are produced from the best available original document.

Efficient broadband second-harmonic generation by dispersive achromatic nonlinear conversion using only prisms

Bruce A. Richman, Scott E. Bisson, and Rick Trebino

Combustion Research Facility

Sandia National Laboratories, M/S 9051

Livermore, CA 94551-0969

Abstract

Using a lossless dispersive apparatus consisting of six prisms, optimized to match a second-harmonic crystal phase-matching angle vs. wavelength to second order, we efficiently doubled tunable fundamental light near 660 nm over a range of 80 nm using a 4-mm-long type-I β -Barium Borate (BBO) crystal. Another lossless set of six prisms after the crystal realigned the propagation directions of the various second-harmonic frequencies to be collinear to within 1/4 spot diameter in position and 200 μ rad in angle. The measured conversion efficiency of a 40-mJ, 5-ns fundamental pulse was 10%.

Acknowledgements

The authors thank Erkin Sidick and Alexander Jacobson of CVI Laser Corp. for their collaboration on the project resulting in this report.

This study was supported by a Sandia Laboratory-Directed Research and Development Grant and by the Office of Basic Energy Sciences, Division of Chemical Sciences, U. S. Department of Energy.

Contents

Nomenclature	6
Introduction	7
Description of the achromatic phase-matching device	9
Characterization of the device	11
Summary	15
References	16

Figures

1 Schematic of the achromatic phase-matching device	10
2 Relative conversion efficiency vs. wavelength and crystal angle	12
3 Relative conversion efficiency at fixed crystal angle	13
4 Position and angle of second-harmonic output beams vs. wavelength	14

Nomenclature

APM	achromatic phase-matching
AR	anti-reflection
BBO	β -Barium Borate
CCD	charge coupled device
DANCE	Dispersive Achromatic Nonlinear Conversion with Efficiency
FWHM	full-width-half-maximum
HeNe	Helium Neon
IR	infra-red
mm	millimeter
μ m	micrometer
mrad	milliradian
μ rad	microradian
Nd:YAG	Neodymium: Yttrium-Aluminum garnet
nm	nanometer
OPO	optical parametric oscillator
SHG	second-harmonic generation
UV	ultra-violet

Efficient broadband second-harmonic generation by dispersive achromatic nonlinear conversion using only prisms

Introduction

Many applications require broadly tunable UV light. No such laser source exists, however, so tunable UV is usually obtained by frequency-doubling a tunable laser in the visible and near-IR. Since frequency-doubling usually involves a nonlinear crystal with a wavelength-dependent phase-matching angle, the crystal must be tilted as the wavelength is tuned¹. Unfortunately, this procedure can be unreliable, despite the use of feedback, and it is sensitive to vibrations. In addition, it produces undesirable beam walk as the laser tunes, which must be corrected with yet another moving part.

Several researchers have introduced achromatic phase-matching (APM) devices that use angular dispersion so that each wavelength enters the nonlinear crystal at its appropriate phase-matching angle. The crystal and all dispersing optics remain fixed. Because such systems have no moving parts, they are inherently instantaneously tunable, and thus can also be used for nonlinear conversion of tunable or broadband (such as ultrashort) radiation. Most of these devices have used gratings or prisms in combination with lenses,²⁻⁵ which have the disadvantage that they are sensitive to translational misalignment. Also, previous work has considered only the lowest order (linear) term of the dispersion and the phase-matching angle tuning function^{2,6}. Bandwidths of ~10 times the natural bandwidth of the crystal have been achieved; larger bandwidths have only been obtained by using a

divergent beam at the expense of conversion efficiency⁵. Also, little attention has been paid to efficiency.

Previously, we⁷ considered the dispersive elements and phase-matching-angle tuning functions exactly using full Sellmeier equations. We used a grism (a transmission grating on the surface of a prism⁸), which has the large dispersion of a grating and, unlike a grating, its dispersion matches the first- and second-order of the crystal phase-matching angle tuning function. Unfortunately, grisms with high diffraction efficiency are not yet available. Indeed, no previous APM device has simultaneously achieved high efficiency and a tuning range greater than 10 times the crystal bandwidth.

In this letter, we describe an APM device made entirely of prisms operating near Brewster's angle or anti-reflection (AR) coated for normal incidence. This device also includes dispersion after the crystal to coalign all of the second-harmonic beams. Using a 4-mm-long type I β -Barium Borate (BBO) crystal, it achieves a bandwidth of 80 nm fundamental wavelength centered at 660 nm—150 times the natural bandwidth of the crystal. Using a 40-mJ, 5-ns pulse from a commercial OPO as the fundamental source, we obtained 10% conversion efficiency over the entire bandwidth. Also, after the crystal, an analogous set of prisms realigns the propagation directions of the various second-harmonic frequencies to be collinear to within 1/4 spot diameter in position and 200 μ rad in angle. Because the acronym "APM" is also used for an unrelated technique (additive-pulse modelocking), as well as for nondispersive broadband frequency-doubling schemes, we call this efficient method "dispersive achromatic nonlinear conversion with efficiency" (DANCE).

Description of the achromatic phase-matching device

A single glass prism has only $\sim 1/10$ the dispersion necessary at the crystal, so ten prisms in series could be used to achieve the required dispersion⁶. This is inconvenient, so we use one equilateral prism followed by three Littrow prisms (30° apex angle), each of which not only adds to the dispersion, but also magnifies it (since compression in space yields increased divergence). The beams enter the Littrow prisms near normal incidence and exit near Brewster's angle ($\sim 60^\circ$). Each Littrow prism spatially compresses the beam in the plane of refraction, which introduces a magnification of the upstream dispersion angle by ≈ 1.8 . Figure 1 is a schematic of the DANCE device, showing the equilateral prism (3) and the Littrow prisms (4, 5, and 6).

We use an additional two prisms (1 and 2) before the equilateral prism to spatially (but not angularly) disperse the beam, so that the angular dispersion introduced by the remaining prisms causes all frequencies to converge, rather than diverge, in the crystal. The first two prisms also solve another problem: the magnification of the Littrow prisms 4, 5, and 6 increases the divergence of the beam at each frequency, possibly beyond the acceptance angle of the BBO crystal. Prisms 1 and 2 are also Littrow, but are oriented to demagnify the beam divergence, partially compensating the magnification of the other Littrow prisms. The long path between prisms 1 and 2 is folded twice by two high-reflectivity mirrors. All of the input prisms are made of SF11 glass except the second prism, which is F2 glass. Its index must be smaller than that of the first prism so that net angular dispersion of the first two prisms is zero.

The polarization through the prisms is chosen to be p since most optical faces are near Brewster's angle, and the remaining faces are AR coated. A $\lambda/2$

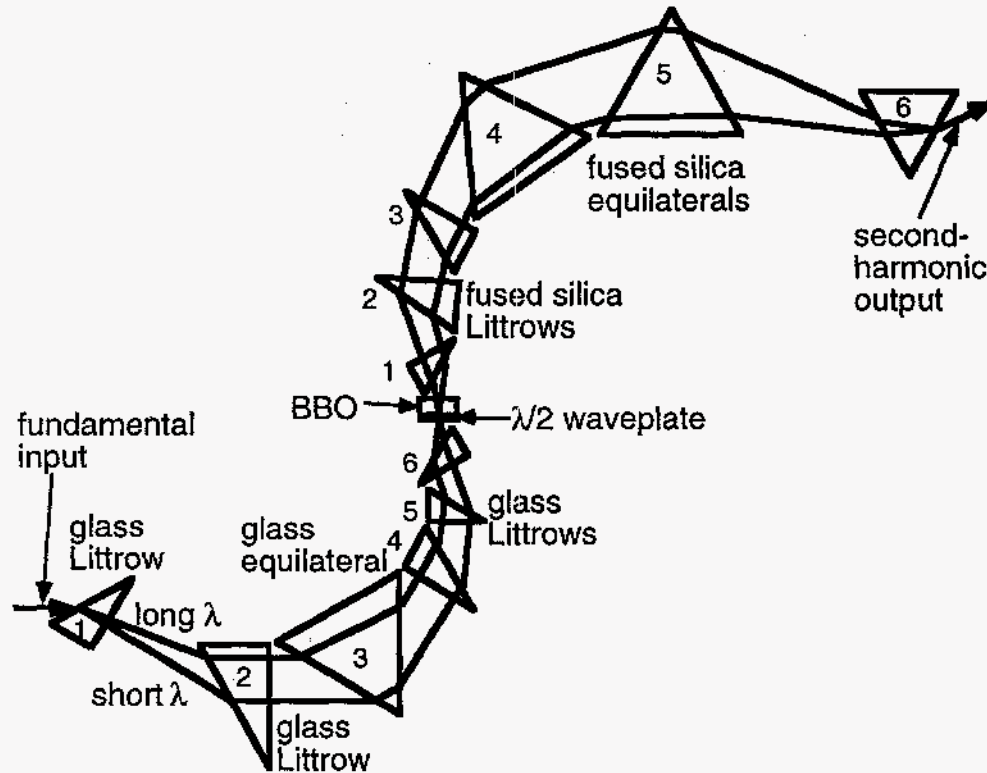


Figure 1. Schematic of the achromatic phase-matching device. The first two prisms disperse the fundamental beam spatially (but not angularly) so that the rest of the prisms cause all beams to converge in the crystal. The 4th 5th, and 6th (Littrow) prisms each have a 30° apex angle, and mostly magnify the dispersion of the 3rd prism. The output side of the DANCE device is qualitatively the reverse of the input.

waveplate is then required just before the BBO crystal to rotate the polarization to s for type I phase-matching.

The output side of the device, after the BBO crystal, is qualitatively the reverse of the input side, but all the prisms are made of fused silica. The apex and incident angles are also different from the input. The last two prisms are not arranged analogously to the first two prisms of the input because they have the same index. They are both Brewster prisms, and do not spatially

compress the beam. No waveplate is needed since the second-harmonic polarization from the crystal is p. Because of the different magnification from the input, the output beam is wider than the input by a factor of ≈ 4 , which we compensated with a cylindrical telescope after the last prism. The spot diameter after this telescope was approximately 1 mm. We used a simulated annealing algorithm⁷ to compute the optimum orientations and incidence angles of each of the prisms in both the input and the output.

Characterization of the device

We characterized our device with a tunable commercial optical parametric oscillator (OPO) pumped with the third harmonic of a Q-switched Nd:YAG laser. Figure 2 shows a density plot of the experimentally measured relative second-harmonic conversion efficiency as a function of wavelength and absolute crystal angle. Each point is an average of the second-harmonic pulse energy divided by the square of the fundamental energy averaged over several laser shots, and then normalized to the maximum value at each wavelength to remove the wavelength dependence of the detector and filters. The plot should consist of a sinc^2 angle tuning curve at each wavelength. Shown for comparison is the computed difference between the predicted DANCE device dispersion angle and the exact phase-matching angle of the BBO crystal. It follows the experimental maxima, as it should. Note that the remaining variation in angle vs. wavelength is third-order. Once the input prisms of the device were pre-aligned to the computed optimum orientations using a red HeNe laser, only one degree of freedom was needed to optimize the dispersion experimentally. This optimization was accomplished by the

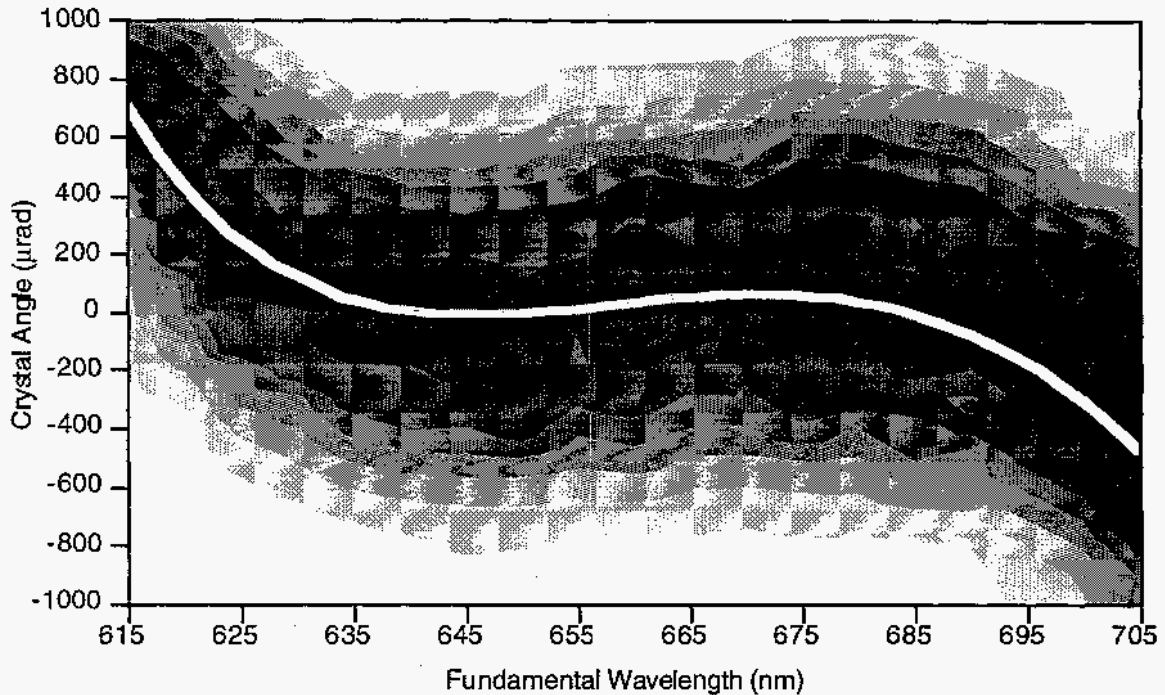


Figure 2. Relative conversion efficiency vs. wavelength and crystal angle.

The contour plot is the experimentally measured small-signal relative second-harmonic conversion efficiency. The solid curve is the theoretically predicted difference between the dispersion and exact phase-matching angles. It should ideally follow the experimental maxima.

adjustment of the angles of prisms 3 and 5, so that the angular positions of the maxima of the sinc^2 angle tuning curves at two well-separated wavelengths matched the computed difference curve.

Figure 3 is a slice of figure 2 at fixed (zero) crystal angle. It shows clearly a full-width-half-maximum fundamental bandwidth of 80 nm. The experimental points agree with the relative conversion efficiency computed from the predicted angle difference curve in figure 2. Shown for comparison is the predicted relative conversion efficiency of a grating operating at the

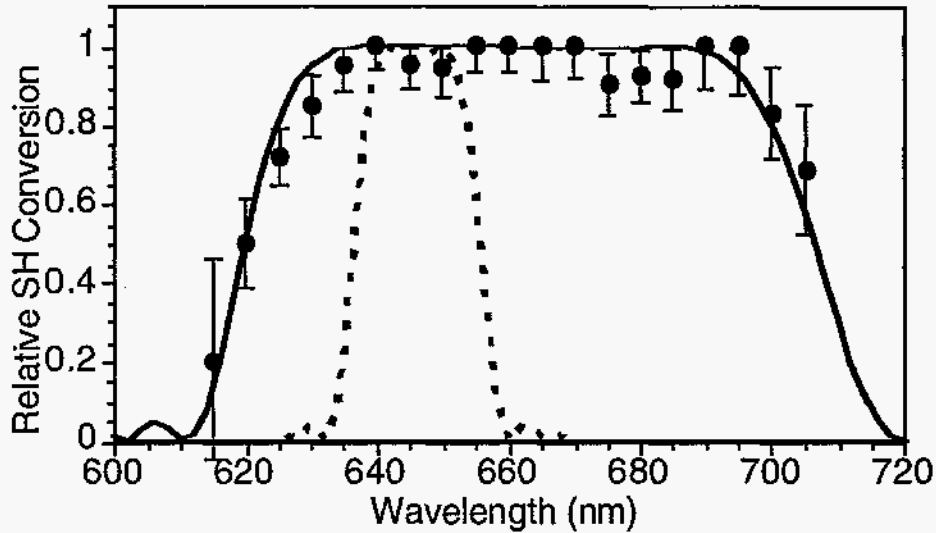


Figure 3. Relative conversion efficiency at fixed crystal angle. Slice of the data in figure 2 at constant (zero) crystal angle, compared with the theoretically predicted relative conversion efficiency (solid curve). Both have a FWHM bandwidth of 80 nm. Also shown is the theoretically predicted conversion efficiency when using a single grating operating at the Littrow condition (dashed curve). Its bandwidth is only 15 nm.

Littrow condition (diffracted angle = - incident angle), with the correct linear dispersion to match the BBO angle tuning curve. Its bandwidth is only 15 nm since it does not match the BBO angle tuning curve beyond first order.

The output of the device was also prealigned with a red HeNe laser. We measured and coaligned the second-harmonic beam positions and angles precisely using lenses to image them onto a CCD array (after the telescope mentioned above). The output prisms were experimentally optimized by adjusting the angle of prism 5 to provide nearly constant output position and

the angle of prism 6 to center the experimental output angle curve with respect to the predicted curve.

Figure 4 shows the measured position and angle (in the dispersion plane) after the last prism as functions of wavelength, and the angle predicted from the computed optimum prism orientations. The position has been normalized to the ≈ 4 mm spot diameter at the exit of the last prism. Each point is the average of 40 laser shots of the centroid of the beam spots on the CCD, taking into account the magnification of the imaging lenses and the telescope. Since the collinearity is quadratically limited (as the theoretical curve is nearly a parabola), the computed parabolic curvature can be achieved only with perfect alignment of all of the output elements. With even slightly imperfect alignment, the achieved parabola will be sharper, as observed.

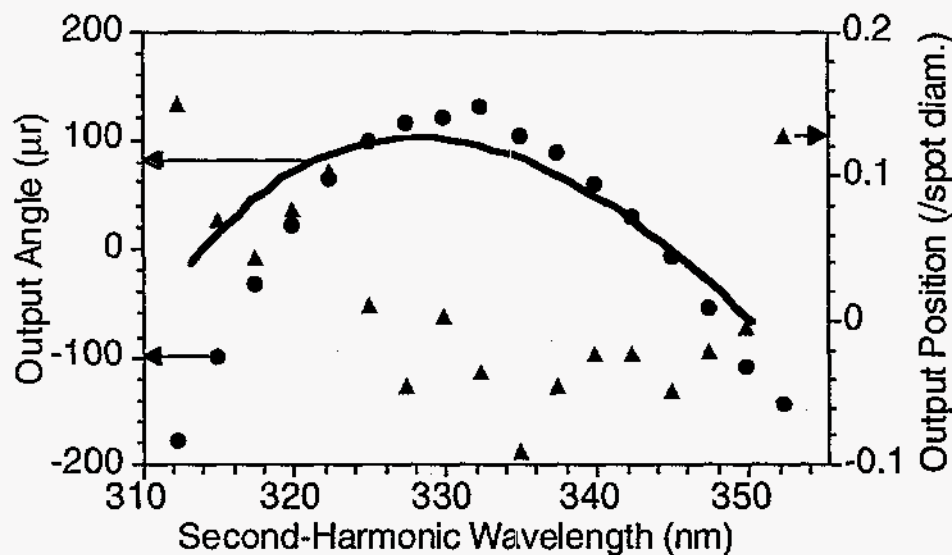


Figure 4. Position (triangles) and angle circles) of second-harmonic output beams vs. wavelength. The second-harmonic beams were observed in the plane of dispersion, at the output of the DANCE device. The solid curve is the model-predicted angle.

The position and angle out of the dispersion plane (vertical) should remain constant over all wavelengths. However, small tilting of a prism can introduce its own vertical dispersion, and couple dispersion from upstream into the vertical plane. We observed a mostly linear dependence of both vertical position and angle on wavelength with slopes of $40 \mu\text{m}/\text{nm}$ and $15 \mu\text{rad}/\text{nm}$ respectively. We believe that one prism is responsible for most or all of this dispersion. In theory, this minor problem is easily compensated by tilting other prisms, but the mounts in the device described here did not permit precise vertical tilting of the prisms.

Summary

We measured a 10% absolute conversion efficiency of fundamental into the second-harmonic over the entire bandwidth except at wavelengths greater than 690 nm because the OPO dichroic mirrors purposely do not reflect well near 710 nm. The conversion efficiency of the same crystal placed directly in the OPO beam was 19%. We believe the discrepancy arose mostly from losses at the many optical surfaces that were not perfectly clean, and the difficulty in orienting the waveplate at the BBO crystal. These problems were peculiar to our prototype design and will be corrected in future designs.

We believe that this is the first complete and practical broadband frequency-doubling device with no moving parts.

References

1. Valentin G. Dmitriev, Gagik G. Gurzadyan, and David N. Nikogosyan, *Handbook of Nonlinear Optical Crystals*, Antony E. Siegman ed., Springer-Verlag, Berlin, 1991.
2. Oscar Eduardo Martinez, Achromatic phase matching for second harmonic generation of femtosecond pulses, in *IEEE Journal of Quantum Electronics*, vol. 25, pp. 2464-2468, 1989.
3. G. Szabo and Z. Bor, Broadband frequency doubler for femtosecond pulses, in *Applied Physics B*, vol. 50, pp. 51-54, 1990.
4. Robert W. Short and Stanley Skupsky, Frequency conversion of broadband laser light, in *IEEE Journal of Quantum Electronics*, vol. 26, pp. 580-588, 1990.
5. Seishiro Saikan, Donald Ouw, and Fritz P. Schäfer, Automatic phase-matched frequency-doubling system for the 240-350-nm region, in *Applied Optics*, vol. 18, pp. 193-196, 1979.
6. V. D. Volosov and E. V. Goryachkina, Compensation of phase-matching dispersion in generation of nonmonochromatic radiation harmonics. I. Doubling of neodymium-glass radiation frequency under free-oscillation conditions, in *Soviet Journal of Quantum Electronics*, vol. 6, pp. 854-857, 1976.
7. Bruce Aram Richman, Scott E. Bisson, Rick Trebino *et al.*, Achromatic phase matching for tunable second-harmonic generation by use of a grism, in *Optics Letters*, vol. 22, pp. 1223-1225, 1997.
8. S. Kane and Jeffrey Squier, Grism-pair stretcher-compressor system for simultaneous second- and third-order dispersion compensation in chirped-pulse amplification, in *Journal of the Optical Society of America B*, vol. 14, pp. 661-665, 1997.

Distribution:

1 MS 9051 Bruce Richman, 8366
1 MS 9051 Rick Trebino, 8366
1 MS 9051 Scott Bisson, 8366
1 MS 0188 LDRD Office
3 MS 9018 Central Technical Files, 8940-2
4 MS 0899 Technical Library, 4916
1 MS 9021 Technical Communications Dept., 8815/Technical Library, 4916
2 MS 9021 Technical Communications Dept., 8815 for DOE/OSTI
1 MS 0161 Patent and Licensing Office, 11500
1 MS 1380 Technology Transfer, 4212

This page intentionally left blank